

# The Magnetized Dusty Plasma Experiment (MDPX)

E. Thomas, Jr.,<sup>1</sup> U. Konopka,<sup>1</sup> D. Artis,<sup>1</sup> B. Lynch,<sup>1</sup> S. LeBlanc,<sup>1</sup> S. Adams,<sup>1</sup>  
R. L. Merlino<sup>2</sup> and M. Rosenberg<sup>3</sup>

<sup>1</sup> *Physics Department, Auburn University*

<sup>2</sup> *Department of Physics and Astronomy, The University of Iowa*

<sup>3</sup> *Electrical and Computer Engineering, University of California – San Diego*

(Received ?; revised ?; accepted ?)

The Magnetized Dusty Plasma Experiment (MDPX) is a newly commissioned plasma device that started operations in late Spring, 2014. The research activities of this device are focused on the study of the physics highly magnetized plasmas and magnetized dusty plasmas. The design of the MDPX device is centered on two main components: a open-bore, superconducting magnet that is designed to produce, in steady state, both uniform magnetic fields up to 4 Tesla and non-uniform magnetic fields with gradients of 1 to 2 T/m and a flexible, removable, octagonal vacuum chamber that provides substantial probe and optical access to the plasma. This paper will provide a review of the design criteria for the MDPX device, a description of the research objectives, and brief discussion of the research opportunities offered by this multi-institution, multi-user project.

## 1. Introduction

The presence of a magnetic field in a plasma physics experiment is well-known to substantially alter the properties of the plasma. A magnetic field can have a dominating influence on a plasma for phenomena ranging from the modification of transport of ion and electrons, the confinement of those plasma particles, and the generation of instabilities.<sup>1</sup> This applies equally to phenomena observed in laboratory,<sup>2</sup> space,<sup>3</sup> and fusion<sup>4</sup> plasmas. Therefore, for almost a century, plasma researchers have been investigating the properties of plasmas under the influence of magnetic fields.

By contrast to the long study of magnetized plasmas, the study of strongly coupled dusty (complex) plasmas has emerged as a unique discipline within the larger community of basic plasma physics. Here, a dusty plasma refers to a four-component plasma systems that consists of electrons, ions, neutral atoms, and charged microparticles (i.e., the "dust") that are suspended in the background plasma. Because these microparticles are charged, they fully interact with and are coupled to the background plasma in a manner that causes new and unique plasma phenomena to arise in the plasma.<sup>5</sup> Moreover, because the microparticles can often be individually tracked in the plasma, dusty plasmas offer the opportunity to study both small scale (kinetic) and large scale (collective) plasma phenomena in a single system.

The history of the observation of particulate matter in plasmas extends to the origins of plasma physics. In a paper in 1927,<sup>6</sup> I. Langmuir reported observations of "globules" in a gas discharge that "move very slowly so that their motions through the arc could be easily followed by the unaided eye" – an observation that mirrors many laboratory dusty plasmas today. In

1956, a paper by Mestel and Spitzer noted the important role that charged magnetized dust could play in the processes that lead to star formation.<sup>7</sup> The modern study of dusty plasmas over the last three decades began in the mid-1980's in the attempts to understand the role of charged, micron-sized dust in the formation of planetary rings<sup>8,9</sup> and extending to understanding dust in the solar system.<sup>10</sup>

At the same time, with the initial observations of the formation of nanometer and micrometer sized dust in plasma processing reactors,<sup>11, 12</sup> it was becoming increasingly evident that it was important to understand how these small particles formed, became charged, remained trapped in the plasma, and self-consistently modified the plasma environment through the introduction of the third charged species. With the laboratory observations of new types of dust-driven plasma instabilities<sup>13, 14</sup> and the ability of the particles to form strongly-coupled, self-organized structures,<sup>15, 16</sup> research in the field of dusty/complex plasma research began accelerating. However, in spite of the substantial growth of the field – the focus of the vast majority of laboratory experiments have focused on particles that were electrostatically confined in the plasma.

It is now understood that the microparticles in dusty plasmas typically are in the size range of tens of nanometers to a few hundred micrometers in diameter and can carry an excess surface charge of a few tens of electrons to many thousands of electrons for larger particles in a plasma environment. Although these particles are often highly charged, their large mass (as compared to the ions and electrons, e.g.,  $10^8$  to  $10^{10}$  ion masses) makes their charge-to-mass ratio very small; for example, for a 1-micron diameter silica dust particle (mass density,  $\rho = 2200 \text{ kg/m}^3$ ) in a typical laboratory argon plasma (electron/ion plasma densities,  $n_e \approx n_i \sim 10^{15} \text{ m}^{-3}$ ; electron temperature,  $T_e \sim 3 \text{ eV}$ , and ion temperature,  $T_i \sim 0.025 \text{ eV}$ ), the charge-to-mass ratio is a factor of  $10^{-12}$  times the electron charge-to-mass ratio. This key fact is the primary reason that developing an experimental system to study the physics of a magnetized dusty plasma - where the electrons, ion, and dust particles are magnetized - is technically challenging.

More precisely, if the Hall parameter (the ratio of the gyrofrequency to neutral damping frequency) for a dusty plasma is considered as a typical criterion for magnetization, it is found that this ratio will scale as:

$$R_{\text{Hall}} = \omega_{cd} / \nu_{dn} \sim B v_{tn} / a P > 1 \quad (1)$$

Here,  $\omega_{cd}$  is the dust cyclotron frequency ( $\omega_{cd} = q_d B / m_d$  – where  $q_d$  is the dust grain charge,  $B$  is magnetic field, and  $m_d$  is the dust grain mass and  $q_d / m_d$  scale as  $a^{-2}$ , where  $a$  is the dust grain radius) and  $\nu_{dn}$  is the dust-neutral damping frequency ( $\nu_{dn} \sim a^2 n_n v_{tn} m_n / m_d$ ; where  $n_n$  is the neutral gas number density, which is proportional to the neutral pressure,  $P$ ,  $v_{tn}$  is the thermal velocity of the neutral gas, and  $m_n$  is the mass of the neutral gas atoms;  $\nu_{dn} \sim a^{-1}$ ).<sup>17</sup> This shows that a combination of large magnetic fields strength, low operating pressure, and small particle size is needed to operate an experiment in a parameter regime where the charged microparticles can be magnetized. These are among the most important considerations that guided the development of the MDPX proposal and in the design of the device and its supporting diagnostic systems. Figure 1 shows a calculation of the Hall parameter and the dust grain charge over a range of particle diameters for typical experimental parameters. It is shown that there exists a reasonable regime of parameter space over which the microparticles are expected to satisfy the magnetization criteria.

The development of the overall MDPX project was done as a community-wide effort led by a multi-institutional team from Auburn University, the University of Iowa, and University of California - San Diego. An earlier paper by Thomas, et al., described the preliminary design and mission of the MDPX device.<sup>18</sup> While the experiment is located on the campus of Auburn University in Auburn, Alabama, it is built upon the experience and expertise of the broader dusty plasma research community whose input were essential to its development. MDPX is designed to extend the previous studies of the coupling between dusty plasmas and magnetic fields.<sup>19,20,21,22,23</sup> What follows in this paper is a description of the MDPX design parameters followed by a brief primer on the anticipated research objectives to be performed using the MDPX device as well as some of the technical challenges and opportunities that will be afforded by this project.

## **2. Machine description**

The MDPX device is composed of several integrated subsystems that must work together seamlessly in order to achieve our research objectives. At time when this paper was being written (July, 2014), the MDPX device has been in operation for approximately six weeks. As such, the experimental configuration and initial operating parameters are based upon the very early operations of the device. Currently, MDPX is in a commissioning phase that is expected to continue through early 2015. Upon completion, full research operations will commence – including collaborative experiments.

The primary subsystems of the MDPX device are: superconducting magnet, vacuum vessel and associated vacuum systems, plasma generation system, experimental control and data acquisition system, and plasma diagnostics. Each of these subsystems will be described in the sections below.

### *2a. Superconducting magnet*

The heart of the MDPX device is the superconducting magnet. The coils and their support systems were designed in a partnership between Auburn University, the MIT Fusion Engineering group, and Superconducting Systems, Inc. (SSI). The coils were manufactured in Billerica, Massachusetts by SSI.

The magnet consists of two coil pairs (a total of 4 coils) contained in an "open-bore" cryostat - with two coils located in each half of a cryostat. The arrangement and designation of the four coils is given in Figure 2a. Each coil is constructed from 1.1 mm diameter wire composed of copper with embedded niobium-titanium superconducting strands. The wire becomes superconducting at a critical temperature of 6.4 K. The dimensions and windings of the four coils are given in table 1. The coils were embedded in epoxy and the first pair were assembled onto an aluminum support structure as shown in figure 2b. The coils and their support structure are all part of the internal cold mass of the magnet. The cryostat is sealed, evacuated, and cooled to cryogenic temperatures using a pair of Sumitomo model RDF-415D (4.2 K, 1.5 W) cryocoolers - one on each side of the cryostat. The magnet is instrumented with a variety of temperature sensors from Lakeshore Cryogenics to monitor the temperatures of the coils, cryocoolers, and the radiation shields. Lakeshore model DT-670-SD silicon diode sensors are used for the radiation shields, while more sensitive model RX-202A-AA ruthenium oxide (ROX) sensors are used to monitor the temperature of the coils. A Lakeshore Model 224 temperature monitor is connected to the sensors and is integrated via a General Purpose Interface Bus (GPIB) interface into the data acquisition system. When cooled, the coils have baseline temperatures

ranging from 4.2 to 4.6 K while the outermost radiation shields (closest to the outer wall of the cryostat) have a baseline temperature in the 60 - 65 K range.

---

Coil	ID (mm)	OD (mm)	Z1 (mm)	Z2 (mm)	Turns
1a	560.5	692.2	468.3	601.0	7068
2a	673.3	913.0	140.4	269.3	12430
2b	673.3	913.0	-140.4	-269.3	12430
1b	560.5	692.2	-468.3	-601.0	7068

---

TABLE 1. Parameters for the MDPX magnetic field coils as measured from the geometric center of the magnet cryostat. ID and OD refer to the inner and outer diameter of the coil, respectively. Z1 and Z2 refer to the axial extent of the coil windings as measured from the geometric center of the magnet ( $Z = 0$  mm).

---

The cryostat has a cylindrical "warm bore" that is 50 cm in diameter and 157 cm axially. Additionally, a unique feature of the MDPX magnet is the use of an "open-bore" design. This is shown in figure 2, which shows a schematic drawing of the magnet and its assembly, and in figure 3, which shows a photograph of the cryostat that contains the magnet. The center of the magnet is open with the exception of four, 15 cm diameter posts centered on a circle of radius of 19.3 cm relative to the center of the magnet. Inside of these posts are stainless steel rods that separate the "a" and "b" sections of the magnet. These rods are part of the cold mass and provide structural support against both compressive and tension forces exerted between the coils. This feature was an important requirement of the research team as it allows radial access to the vacuum chamber and facilitates extensive diagnostic access to the plasma. Additionally, along each of the flat surfaces of the cryostat (i.e., top and bottom of both the "a" and "b" sections), there is an extensive array of tapped mounting points using helicoils that use a combination of 1/4"-20 and 3/8"-16. The use of the 1/4"-20 mounting points is particularly helpful as it provides convenient locations for attaching optical components.

The electrical system for the magnet is based upon the use of a single power supply to provide current to all four coils to produce a "symmetric" magnetic field and then using three smaller power supplies to produce an "anti-symmetric" configuration. The symmetric configuration is the default operational mode used to produce a uniform magnetic field at the center of the MDPX device. The combination of the two configurations is designed to produce a variety of non-uniform magnetic field structures; this is another unique feature of the MDPX device. To date, commissioning experiments have focused on producing uniform magnetic fields in MDPX. However, early tests have shown that the magnet is capable of operating in a non-uniform mode, but extensive testing has not yet been performed. Non-uniform magnetic field configurations will be studied later in the commissioning phase, towards the end of 2014 or early 2015 and will be discussed in future publications.

To produce a uniform magnetic field, the magnet is powered using a TDK Lambda Genesys GEN8-180 (180 A / 8 V) power supply. At a full current of 127.5 A, the magnet is designed to produce a magnetic field of 4 Tesla at the center of the MDPX device. The magnet has a uniform region at the center of the magnet that extends 20 cm in diameter and 5 cm in the axial direction. In this region, the magnet is designed to have a variation of under 1% as defined by Eq. 2.

$$\varepsilon = \frac{(B_{\max} - B_{\min})}{\frac{1}{2}(B_{\max} + B_{\min})} \quad (2)$$

A contour plot of the measured magnet field in the central gap of the warm bore is shown in figure 4 when the magnet was operated in a uniform mode with a nominal field strength of  $|B| = 0.5$  Tesla. From these measurements, an estimate can be made of the magnetic field variation in both the radial and axial directions. It is shown the  $\varepsilon_{\text{radial}} \sim 0.95\%$  and  $\varepsilon_{\text{axial}} \sim 0.45\%$ . As of the writing of this paper, the magnet has been successfully tested up to magnetic fields of 2 Tesla and the coil manufacturer has provided a testing protocol to increase the magnetic field to its maximum value over the next 9 to 12 months.

## 2b. Vacuum chamber and vacuum systems

The next major component of the MDPX device is the vacuum chamber. The vacuum chamber is composed on an octagonal frame that has a maximum outer diameter of 43.2 cm (17"), a circular inner diameter of 35.5 cm (14"), and a height of 17.8 cm (7"). Each face of the octagon has a length of 16.5 cm (6.51") and a rectangular thru-hole that is 12.7 cm tall x 10.2 cm wide (5" x 4"). Custom flanges are attached to each face that adapt to a variety of standard quick-flange and ISO vacuum fittings: QF25, QF40, and ISO63. The side faces can also have windows mounted to them to allow the interior of the vacuum chamber to be viewed.

The octagonal frame is mounted onto a pair of top and bottom flanges that have an outer diameter of 45.7 cm (18") and a thickness of 2.5 cm (1"). These flanges each have a custom thru-hole port at their center with a 14 cm (5.5") diameter. This port is designed to interface with 76.2 cm (30") long extensions that allow the potential plasma volume to extend up to almost 175 cm along the magnet rotational axis. Alternatively, a window could also be mounted on this port to view the interior of the vacuum chamber. The top/bottom flanges also have four QF25 ports equally spaced on a nominal 28.6 cm (11.25") diameter circle. The octagonal frame has O-ring grooves with an inner diameter of 36.2 cm (14.25") at the top and bottom surfaces to interface with top and bottom flanges. Several different views of the MDPX vacuum chamber are shown in Figs. 5(a) to (c).

A vacuum is established using a combination of an Agilent (Varian) Turbo V 81-T turbomolecular pump with an ISO63 inlet backed by an Agilent DS202 two-stage rotary vane pump. Because of the large magnetic field, it is necessary to place the pumps some distance away from the vacuum chamber. A combination of flexible and straight sections of ISO63 tubing extends approximately 6.2 m (20 ft.) between the vacuum chamber to the pumping station. With this configuration, a base pressure  $p \sim 4$  mTorr can be maintained in the MDPX vacuum chamber. Remotely controlled pneumatic valves are used to control which of the pumps, the turbopump or roughing pump, is acting upon the chamber. In particular, for experiments that operate with gas pressures above  $p = 6.7$  Pa (50 mTorr), it is preferable to operate the vacuum system using only the roughing pump.

Gas is delivered to the vacuum chamber using a MKS model 1179A mass flow controller with a 100 sccm (standard cubic centimeter per minute) flow rate for argon. The gas flow rate is set by a 0 to 5 volt signal that is applied from the control computer. In the future, it is planned to operate the experiment with two separate gas input lines. This would allow specific types of gas

mixtures – for example, with silane<sup>24</sup>, or acetylene<sup>2526</sup> gas – in order to perform experiments with growing dust particles.

At the present time, the laboratory at Auburn has two versions of the MDPX vacuum chamber. One is currently installed in the magnet (main experiment chamber) and the other (test stand chamber) is set up in an adjacent laboratory and is being used for diagnostic development and equipment testing. A third version of the vacuum chamber is located at the University of Iowa.

## 2c. *Plasma generation*

For current experiments, a pair of 34.2 cm (13.5”) diameter aluminum electrodes, separated by 6.2 cm (2.45”) are used to generate argon plasma either using a rf or dc glow discharge, parallel plate configuration. The lower electrode has a 0.32 cm deep, 15 cm diameter (1/8” deep by 6” diameter) depression that is designed to aid in the radial confinement of a dusty plasma. The upper electrode has a 14.6 cm (5.75”) diameter through hole that is covered by a thin, tungsten mesh. This hole allows a camera to view the interior of the vacuum chamber from the top.

For rf generated plasmas, a 100 W, 13.56 MHz, fixed frequency radio frequency (rf) generator/amplifier from RF VII, Model RF-3-XIII, is used. The applied rf signal passes through a model ATN-5 auto-tuning matching network with controller and is delivered to the lower electrode in the vacuum chamber; the upper electrode is grounded. Current experiments typically use between 1 and 20 Watts for plasma generation. It is anticipated that future experiments may also use a push-pull mode for the rf generated plasmas where both the lower and upper electrodes are powered.

For dc generated plasmas, a 5 kV, 25 mA dc Glassman, high voltage power supply, Model EH05, is used. Presently, the upper electrode of the MDPX main experiment chamber can be connected to the dc power supply. Here, the DC voltage is not used as a primary plasma source, but rather an auxiliary source used to provide additional control over plasma parameters – particularly the plasma potential profile – which can be useful in modifying and controlling where the dust particles can become trapped in the plasma. This is indicated in figure 7, which shows a schematic drawing of the electrodes and the approximate location of dust trapping in the experiment. On the test stand chamber, the dc glow discharge technique is the primary plasma generation source. As with the vacuum system, the plasma generation systems are all remotely controlled.

The decision to begin experiments using rf and dc generated plasmas using a parallel plate configuration is a legacy that is based upon the experimental configurations that have been extensively tested throughout the three-decade history of laboratory dusty plasma research. A summary of the expected plasma parameters in the MDPX device for rf generated plasmas is given in table 2. It is anticipated that over the lifetime of the experiment, a number of different plasma generation approaches may be used. In particular, consideration was given to a Q-machine type plasma source<sup>27</sup> because of the ability to produce plasmas with equal ion and electron temperatures – which could potentially have interesting effects on the dust grain charge. Another alternative would be to use an inductive, instead of capacitive, rf generated plasma approach in order to decouple plasma production from the use of biased electrodes to control potential structures in the plasma.

---

**Experimental settings:**

Gas:	Argon	Base pressure:	5 mTorr (0.66 Pa)
RF frequency:	13.56 MHz	Operating pressure:	20 to 250 mTorr (2.6 to 33 Pa)
RF power:	2 to 10 Watts	Magnetic field:	0 to 4 Tesla

**Plasma parameters:**

Electron temperature:	2 to 4 eV	Ion temperature:	0.025 eV
Electron density:	$0.2 \text{ to } 1.5 \times 10^{16} \text{ m}^{-3}$	Ion density:	$0.2 \text{ to } 1.5 \times 10^{16} \text{ m}^{-3}$
Electron Debye length:	$\sim 0.4 \text{ mm}$	Ion Debye length:	$\sim 0.04 \text{ mm}$
Electron gyroradius (1 T):	$\sim 0.0004 \text{ mm}$	Ion gyroradius (1 T):	$\sim 0.1 \text{ mm}$

Ion-neutral mean free path:  $\sim 0.06 \text{ mm}$  (@ 10 mTorr)

Ion-neutral mean free path:  $\sim 0.6 \text{ mm}$  (@ 100 mTorr)

**Dusty plasma parameters:**

Dust particles:	silica microspheres	Mass density:	$2200 \text{ kg/m}^3$
Number density:	$\sim 10^9 \text{ to } 10^{10} \text{ m}^{-3}$	Inter-particle spacing:	0.2 to 0.3 mm

Dust particle radius:	$0.5 \text{ }\mu\text{m}$	Charge (@ $0.5 \text{ }\mu\text{m}$ ):	2100 electrons
Dust particle radius:	$0.25 \text{ }\mu\text{m}$	Charge (@ $0.25 \text{ }\mu\text{m}$ ):	1040 electrons

TABLE 2. Estimated parameters for MDPX operations. The experimental settings and the plasma parameters are based upon preliminary single and triple Langmuir probe measurements recorded without a magnetic field ( $B = 0$  Tesla). Dusty plasma parameters are estimates based upon the plasma conditions and without modification of charging due to magnetic field effects.

---

## 2d. *Experimental control and data acquisition*

Experiment control and data acquisition are both enabled through the use of hardware and software from the company National Instruments (NI). A Windows-based PC running the NI *LabVIEW* software is connected to an 18 slot, NI Model PXIe-1075 PXI Express chassis. This provides the hardware interface to the various control and monitoring systems that enable the operation of the experiment as well as allowing measurements, i.e., data acquisition (DAQ) to be performed by the various diagnostic systems. The basic structure of the data system is illustrated in figure 8.

For this experiment, control and monitoring refers to the various subsystems that are needed to generate a magnetic field and produce a plasma. This includes controlling the various pneumatic valves, mass flow controllers, and the turbopump for the vacuum system, controlling the rf and dc power supplies for plasma generation, and controlling the charging current and voltage of the magnet. These systems also monitor the “state” of the experiment; i.e., pressure in the vacuum chamber, temperature of the magnets, the magnetic field, and records view from various overview cameras. The hardware needed to perform these tasks include a PXI-6229 card that provides 16 analog input (AI) and 4 analog output (AO) channels at 250 kilosamples/s (kS/s), a PXI-6224 that provides 16 AI channels at 250 kS/s, a PXI-6723 card that provides 32 AO channels at 800 kS/s, and a PXI-6513 card that provides 32 channels of digital input/output (DIO).

Data acquisition refers to the experimental subsystems that record scientific measurements from the experiment. This primarily refers to measurements obtained from the various diagnostic systems described in section 2e. For data acquisition, the experiment uses a NI PXIe-6363 card with 16 AI and 4 AO channels at 1 megasample/s (MS/s), a PXIe-6124 card with 4 simultaneous sample and hold, 4 MS/s AI channels and 2 AO channels, and a USB-6229 with 16 AI and 4 AO channels at 250 kS/s. Additionally, a PXI-8430 card provides 4 channels of RS-232 communications, a PXI-8252 card provides 3 channels of Firewire (IEEE-1394a) communications, and a PXI-GPIB card provides an interface to GPIB-based instruments (e.g., digital oscilloscopes, current meters, etc.).

Both the control and monitoring systems and the data acquisition systems are monitored using a *LabVIEW* control program. This program, which was developed by our research team, provides a real-time summary of the operation of the experiment. Figure 9 shows a snapshot of the front panel of the control program. This shows the concise manner in which *LabVIEW* can be used to provide an operator of the MDPX experiment an overview of the state of the device.

## 2e. Diagnostics

To complete this section, a brief summary of the diagnostic systems that will be used for the MDPX experiment is given. It is noted that many of these diagnostics are still in their planning stages and have not yet been fully implemented on the experiment. The first four systems discussed below – probes, spectroscopy, laser induced fluorescence, and high speed cameras are planned to be incorporated into the *LabVIEW* data acquisition system. The remaining two systems, particle image velocimetry and real-time imaging and particle tracking, are initially considered as stand-alone systems, but may be integrated at some future time.

1) In-situ probes – These will consist of a typical suite of Langmuir probes – single, double, and triple probes – that have been used extensively for determining the plasma density, electron temperature, and plasma potential of many laboratory plasma experiments. Our group has extensive experience with these types of probes through a variety of laboratory<sup>28,29,30</sup> and fusion<sup>31</sup> experiments. Various texts<sup>32,33</sup> have shown that in the presence of a magnetic field, the transport of ions and electrons to probe surfaces will be modified because transport perpendicular to magnetic field lines will become restricted. This means that the screening length (i.e., the sheath scale length) in the vicinity of the probe will become dependent upon the orientation of the probe surface relative to the magnetic field direction.<sup>34</sup> As a result,

2) Emission spectroscopy – Because of the anticipated difficulties that will arise with probes, a number of alternative, non-invasive diagnostic approaches are under consideration. One of the most important of these will be emission spectroscopy. The emission lines from the plasma provide us information on the magnetic field, due to splitting of atomic lines caused by the Zeeman effect. Because the plasma density is sufficiently low, it should not substantially modify the vacuum magnetic field and therefore the Zeeman effect measurements will provide an alternative method of measuring the peak operating magnetic field of MDPX because most cost-effective, commercial Hall sensors are limited to a maximum magnetic field of 3 Tesla.

Calculations of this size of the Zeeman effect on argon emission lines were done in collaboration with the atomic physics group at Auburn University and preliminary results are shown in figure 10. To detect these effects, the laboratory has access to a McPherson 1.33 m, Czerny-Turner monochromator that has a wavelength resolution of  $\pm 0.5$  Å. This should provide sufficient resolution to resolve the splitting of the lines. Furthermore, we are also working with



the atomic physics group to identify density and electron temperature sensitive lines in argon in order to use emission lines as a plasma diagnostic.

3) Laser induced fluorescence (LIF) – LIF is an optical diagnostic technique in which an injected laser beam is used to optically pump a metastable state in target atomic population. The pumped upper quantum level spontaneously decays-- thus emitting a fluorescence photon. The measured intensity of the fluorescence radiation is a measurement of the target particles velocity distribution. From the width of the obtained distribution –assuming that Doppler broadening is stronger than other broadening mechanisms (such as Zeeman effects), the populations temperature can be extracted from the full width half maximum of the fluorescence signal. In cases where Zeeman effects become significant, one must modify the analysis technique to include the (formerly) higher order effects. Similarly, from the measured peak shift relative to that of the known transition in the particles rest frame, the drift velocity may be obtained. The MDPX LIF system is currently configured to observe the ArII pump transition at 668.6138nm using a Toptica TA Pro 100 diode laser that is tunable over a range from 665-672nm with a mode hop free tuning range of 20-30 GHz.

4) High speed cameras – As with many other dusty plasma experiments, the imaging of the charged microparticles is one of the most essential diagnostic tools. Often, this is done using cameras with frame rates that range from 30 frames per second up to 1000 frames per second. Cameras based upon both CCD and CMOS sensors have been successfully used for unmagnetized experiments. It remains to be seen which cameras will be able to operate in the high magnetic field environment of MDPX. So far, in the initial experiments, a USB2-based, 50 frame per second, 752 by 480 pixel, IDS Model uEye LE industrial camera and a USB3-based, 90 frame per second, 2048 by 2048 pixel, Ximea model xiQ camera have been used to image the dusty plasmas. An example of a dust cloud imaged through the top window of the vacuum chamber is shown in figure 11.

5) Particle image velocimetry (PIV) – PIV is an image analysis technique that has been used extensively by the Auburn group for over a decade to perform planar<sup>35,36</sup> and stereoscopic<sup>37,38</sup> measurements of dusty plasmas. In PIV, an image is decomposed into a grid of cells. The motion of a small group of particles within each cell is determined from their displacement between two sequential images. The motion analysis is performed using a cross-correlation analysis so that individual particles are not tracked from image to image. The source images for PIV can either be obtained from a dedicated hardware system or the analysis algorithm can be applied to an image sequence obtained using a high speed video camera. The images are then analyzed using the Data Visualization (*DaVis*) software package from LaVision, Inc.<sup>39</sup> For the MDPX experiment, we plan to have available a dedicated camera to planar PIV. In time, we hope to also develop a stereoscopic PIV system using cameras that are compatible with the high magnetic field environment.

6) Real-time imaging and particle tracking – An important diagnostic tool that will be used for this project will be real-time imaging and particle tracking using the Complex Plasma Analysis (*CoPIA*) software package. *CoPIA* is as a Linux-based program originally designed to control hardware of micro-gravity based complex plasma experiments.. Unlike the proprietary software packages (e.g. *DaVis*), *CoPIA* has been developed using solely open source libraries, which permit the public release of source code. We plan to release *CoPIA* to the public under an open source license so that the source code may be freely modified and adapted to meet the specific needs of the user. For the MDPX experiment, the *CoPIA* software has been updated to include “real-time” Particle Tracking Velocimetry (PTV) analysis calculations of dust cloud

dynamics. The newly developed PTV software features a shared memory interface between the imaging data and PTV analysis, which means that data can be analyzed without first being recorded to disk. This functionality provides users with a way to select desirable dust cloud conditions by fine tuning plasma parameters before large amounts of unnecessary data is recorded. The software also includes custom graphics rendering (using OpenGL) of both the recorded images and also display of the extracted velocity fields. The velocity fields extracted using PTV provide a temporally and spatially resolved particle phase-space distribution function (PSD), which can be used to calculate thermal properties of the system (i.e. pair correlation functions and kinetic temperatures). The fast calculation and graphics rendering of thermodynamic quantities is still under development and is expected to be completed over the next year. When applying particle tracking velocimetry techniques to MDPX, the addition of an external magnetic field is expected to significantly modify not only the global dust cloud PSD but also single particle motion. In particular, the PTV technique is preferable to the Particle Imaging Velocimetry (PIV) technique in situations where the dust cloud flow density is low or when examining single particle dynamics.

### **3. Research objectives**

As discussed in the introduction, achieving the experimental conditions necessary for achieving a magnetized dusty plasma can be challenging. However, if a laboratory experiment can be made that can achieve these experimental parameters, this not only opens new opportunities for the study of dusty plasmas, it also offers the opportunity to investigate fundamental plasma physics (i.e., without the presence of dust) in an operational regime that has not been extensively investigated experimentally. Therefore, we believe that the MDPX project offers great promise as a platform to study a variety of plasma phenomena.

The primary mission of the MDPX project is the study magnetized dusty plasmas. This is summarized in the scientific mission of the project: to study the structural, thermal, and stability properties of a dusty plasma in which the magnetic force acting upon each of the charged plasma components is comparable to the electrical, gravitational, or inter-particle forces. That is, the magnetic force must be a significant contributor to the overall force balance for each charged species in the plasma. Within this overarching mission, the two main goals of the project are to: (1) Investigate how the structural, thermal, charging, and stability properties of a dusty plasma evolve as the system is taken from an unmagnetized state through a progression of regimes where first the electrons, then the ions, and then charged microparticles become magnetized; and (2) Investigate how the properties of a dusty plasma composed of microparticles that have paramagnetic or ferromagnetic properties evolve in the presence of uniform and non-uniform magnetic fields.

It is possible to imagine a broad range of experimental investigations that fall within the purview of the two goals listed above. Within the dusty plasma research community, there have been numerous discussions on the impact of the magnetic field on dusty plasma instabilities, the formation of strongly coupled systems, phase transitions, voids, and a wide variety of other phenomena. In this brief primer, two fundamental questions are highlighted that lie at the core of all of the processes that affect the behavior of the dusty plasma:

- (1) How is the dust grain charge affected by the magnetic field?
- (2) How are the inter-dust forces modified by the magnet field?

It is well known that the dust grains collect ions and electrons from the plasma. This grain charge is necessary to allow the dust particles to remain suspended in most laboratory plasmas. In the absence of a magnetic field, the grains will acquire a net negative charge under typical laboratory conditions. The current understanding of dust grain charging suggests that charging can either be an isotropic process when grains are levitated in the bulk plasma or affected by ion flows when grains are levitated near a plasma sheath. In the presence of a magnetic field, the ion and electron dynamics will become significantly restricted as cross-field transport is inhibited by a large magnetic field, but it remains unclear how this will impact the grain charge. Theoretical studies by Tsytovich, et al.,<sup>40</sup> and Chang and Spariosu<sup>41</sup> suggest that there will be an evolution of the grain charge as a function of increasing magnetic field.

Given the challenges associated with probe measurements in strong magnetic fields, as discussed briefly in section 2e, and the fact the probe measurements in the vicinity of a dusty plasma are known to be highly perturbative to the dust particles<sup>42,43</sup> it is not surprising that, at the present time, no experimental measurements have been reported on the dust grain charge in a strongly magnetized plasma. As a result, understanding how the magnetic field alters the charging process, modifies the equilibrium charge of the dust grains, and therefore alters the equilibrium confinement of the grains in the plasma is not only fundamental to understanding the properties of a magnetized dusty plasma, but also an important unresolved experimental issue. For the MDPX project, a combination of measurements of the dust and plasma parameters without a magnetic field, modeling, and observations of particle trajectories (e.g., gyromotion or particle deflections due to  $\vec{v} \times \vec{B}$  motion) at high magnetic fields will be used to extract information about the particle charge.

As important as it is to understand how the microparticles become charged, it is equally important to understand the inter-particle forces that control their dynamics. Through many experiments, it has been shown that the dust particles often interact via a screened electrostatic potential, the Yukawa potential.<sup>44,45</sup> However, this screening is assumed to be isotropic in space. In the presence of a magnetic field, the ions and electrons will have a much higher mobility in a direction parallel to the magnetic field as compared to the directions perpendicular to the magnetic field. As with the charging discussed above, this suggests that the Debye screening of the dust grains will become enhanced along the magnetic field direction and reduced in the direction perpendicular to the magnetic field. This potentially creates a spatial asymmetry in the Yukawa interaction between the grains and the wake potential behind the grains.<sup>46,47</sup> Precisely how this asymmetry will manifest itself, for example, by modifying the spatial ordering that is a feature of dusty plasma systems, modifying the role of dust-dust collisions, or by changing how dust driven instabilities propagate throughout the plasma, will need to be explored in greater experimental and theoretical detail.

These two questions in no way represent the diversity of dusty plasma research topics that can be investigated with the MDPX device. Beyond these fundamental questions on dusty plasma properties, applied studies on particle growth and breakup in magnetized plasma, the alignment and confinement of non-spherical dust particles in strong magnetic fields, the transport of charged dust grains in non-uniform magnetic fields, and the properties of dusty plasmas that contain mixtures of non-magnetic and magnetic particles are topics that have relevance to the basic plasma, fusion plasma, and space plasma research communities.

Beyond the study of dusty plasmas, the MDPX device is a unique research instrument for experimental plasma physics. From its inception, MDPX has always been envisioned as a flexible, multi-user, research device. This vision has had a profound impact on the design

criteria of the experiment – pushing it in the direction of the “open bore” approach to maximize probe and optical diagnostic access to the plasma volume. The vacuum chamber is mounted to the magnet via a relatively simple eight-bolt system that is integrated into the top/bottom flanges that allows rapid insertion and removal of the chamber. Moreover, using the top/bottom flanges as a template, other vacuum chambers, for either plasma or dusty plasma experiments, can be quickly exchanged. We believe that this flexibility, combined with the potentially large plasma volume, will make the MDPX device an attractive platform for performing a variety of experiments.

The commissioning studies planned for the MDPX device will focus on determining the operating regime for the experiment. These studies will consider variations in electrode spacing, rf power, and gas pressure in order to establish a wide operating space for studies of dusty plasmas. Beyond this commissioning phase, there are two important baseline studies that are envisioned. The first of these will be to definitively demonstrate that charged microparticles can become magnetized in a laboratory plasma. Ideally, this experiment will consist of introducing a few ( $\sim 10$  to  $100$ ) particles into the plasma and tracking their trajectories over increasing magnetic field. The goal would be to identify dust particle gyromotion or a combination of gyromotion and particle drifts (e.g.,  $E \times B$  drift) that would indicate that the particles are magnetized.

The second baseline study that is envisioned would be to investigate how of the most fundamental modes of a dusty plasma – the dust acoustic wave (DAW) – is affected by the magnetic field.<sup>13</sup> The DAW is understood to be driven by an ion-dust streaming instability.<sup>48</sup> Here, it is possible to explore both the effects of strongly magnetized ions and then magnetized ions and dust grains on the properties of the DAW. Because this wave mode appears in many laboratory experiments and is predicted to occur over a wide range of astrophysical conditions, exploring the properties of the magnetized dust acoustic waves is expected to be of great interest.

In addition to studying magnetized dusty plasmas, MDPX is intended to produce steady-state plasmas at high magnetic fields for extended periods of time; this can be done because of the use of superconducting magnets. This provides an opportunity to investigate the physics of plasmas containing highly magnetized ions and electrons with detailed spatial and temporal resolution. While the plasma density and ion/electron temperatures in MDPX are not compatible with fusion core conditions, they are somewhat representative of the fusion edge plasma. And, MDPX can operate at magnetic fields that comparable to the ITER outer edge magnetic field  $B \sim 5$  T.<sup>49</sup> Thus, it may be possible to consider future MDPX studies that investigate long-duration plasma-wall interactions under magnetic field conditions that may be of interest to fusion studies.

Finally, it may also be possible to access regions of plasma parameter space that are generally poorly diagnosed because of the technical challenges of performing experiments; e.g., regimes of low plasma density and high magnetic field such that the ion cyclotron frequency can be made greater than the ion plasma frequency. Exploring the properties of the plasma and characterizing plasma instabilities in these regimes may yield new insights about the physics of plasmas that could be applied to astrophysical systems where low density plasmas and magnetic fields are present.

#### **4. Technical challenges and opportunities**

The MDPX project presents both opportunities for new scientific discoveries to be made while also presenting a variety of technical and operational challenges to be overcome. An early

operational challenge to be addressed is the use of the MDPX as a multi-user research instrument. The development of the MDPX project was predicated on a multi-user model and the entire core research team is strongly committed to working with the entire plasma physics research community to make this mode of operation a reality. This presents an opportunity to broaden the variety of experiments and experimental approaches beyond those envisioned by the core research team and to leverage the substantial technical and financial investments that have already been put into the MDPX project.

Among the technical challenges is the development of new operating approaches for high magnetic field experiments that maximize experimental performance while minimizing the possibilities of injury to personnel and damage to equipment. For example, even in these initial stages of operation, we have had to develop experimental approaches for linear and rotary motion drives because the large magnetic field can adversely impact the performance of stepper motors. Alternative design approaches, for example, using 3D printed plastic parts for laser and lens holders have already shown great promise for providing new ways of interfacing with the high magnetic field environment of the MDPX device and may lead to the development of new plasma diagnostic tools that can be applied to a variety of basic plasma science experiments.

Beyond the engineering requirements needed to operate diagnostics in a high magnetic field environment, substantial revisions to the theoretical interpretation of diagnostic measurements will need to be developed. The *preliminary* operation of the MDPX device has been in a regime with gas pressures,  $p \sim 2.7$  to 27 Pa (20 to 200 mTorr) and plasma densities,  $n_e \sim 10^9 \text{ cm}^{-3}$ , suggesting a regime of plasma operation that is dominated by collisions with neutral atoms. In this regime, there is limited theoretical guidance the collection of ions and electrons by in-situ diagnostics in the presence of a strong magnetic field. Thus, it will be necessary to develop new physics models and to test the validity of those models in MDPX. These new models may give new insights for understanding how the grains in a dusty plasma become charged in a strongly magnetized plasma as well as providing new methods for interpreting probe measurements in magnetized plasmas.

## 5. Summary

The MDPX device is a multi-user, high-magnetic field research instrument for the study of highly magnetized plasmas and magnetized dusty plasmas. Through the combination of four, superconducting magnetic field coils that can produce a variety of magnetic field configurations from uniform to cusp-shaped magnetic fields, an octagonal vacuum chamber with substantial diagnostic access, and growing set of in-situ and optical diagnostic tools, this newly operating basic research device seeks to explore the physics of plasmas in regimes that have rarely been studied experimentally.

## Acknowledgements

The construction of the MDPX device is supported by a National Science Foundation – Major Research Instrumentation (NSF-MRI) award, PHY-1126067. The operation of the MDPX device is support by grants from the U. S. Department of Energy, DE-SC0010485, and the National Science Foundation, PHY-1301881. The authors thank N. Ivan Arnold and Profs. Stuart Loch and Connor Ballance of the Auburn University Physics Department for their assistance with atomic physics calculations for this project.



Figures:

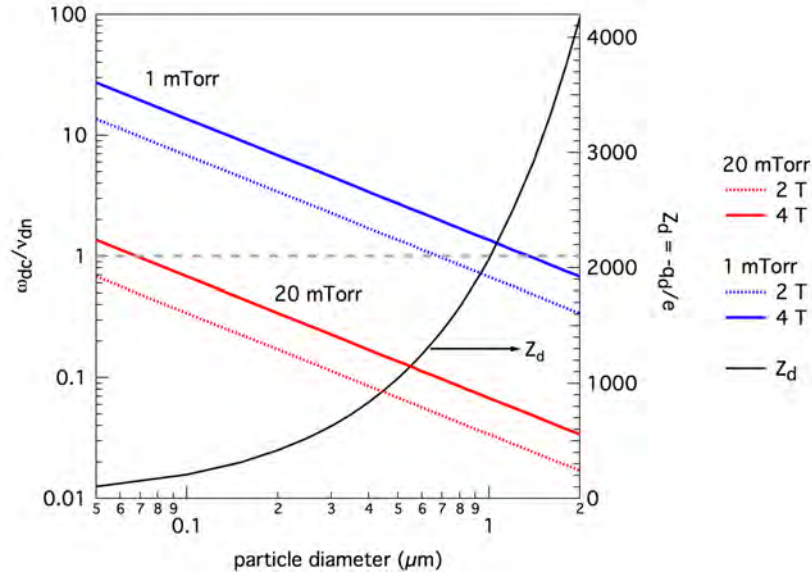


Figure 1: Magnetizing a charged dust particle in a plasma. Calculation of the Hall parameter ( $\omega_{cd}/v_{dn}$ ) as a function of particle size for different neutral pressures (1 and 20 mTorr) and different magnetic fields (2 and 4 T). On the left axis, the Hall parameter is plotted using a log scale. On the right axis, the dust grain charge is estimated and plotted on a linear scale. The horizontal axis shows the particle diameter from 0.05  $\mu\text{m}$  to 2  $\mu\text{m}$  on a log scale. It is assumed that the particles are silica microspheres with a mass density of 2000  $\text{kg}/\text{m}^3$ .

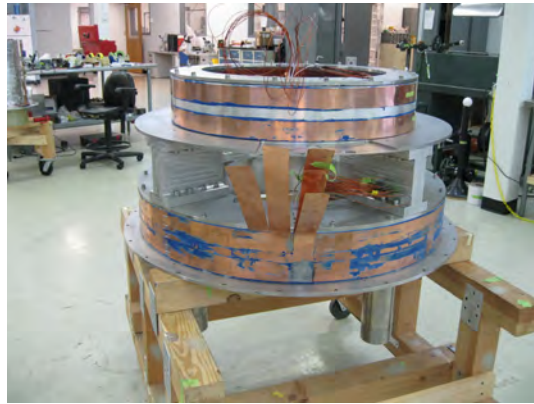
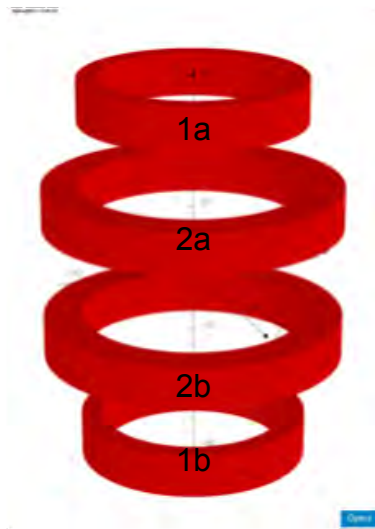


Figure 2: (a) The layout and designation of the four MDPX magnet coils. Coil-type 1 is the smaller coil, while coil-type 2 is the larger coil. The "a" coils are the upper half of the cryostat and the "b" coils are in the lower half.





Figure 3: A photograph of the MDPX cryostat after installation at the laboratory at Auburn University, but prior to the installation of the vacuum chamber. The upper and lower cryostat are visible as are the four posts that separate the upper and lower sides.

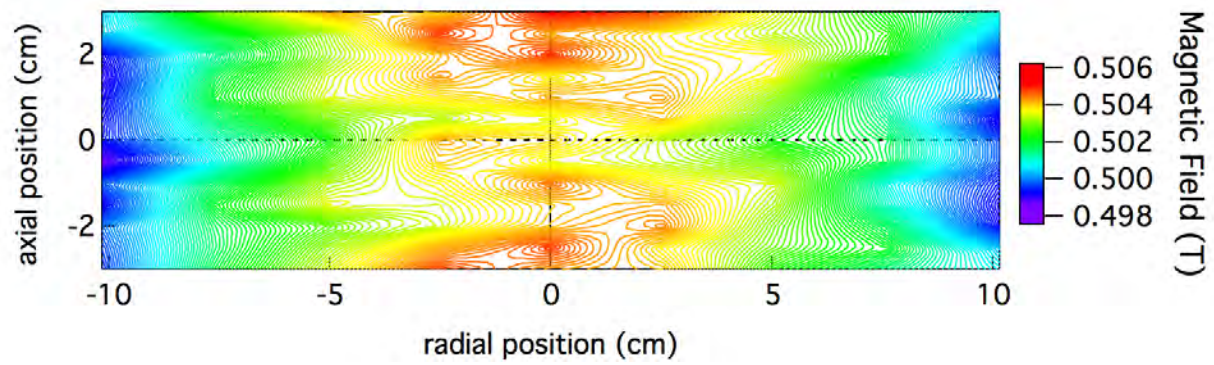


Figure 4: Contour plot of the measured magnetic field of the superconducting magnet for a nominal field strength of 0.5 Tesla. This is a cross-section of a 6 cm axial, 20 cm diameter cylindrical region at geometric center of the magnet.

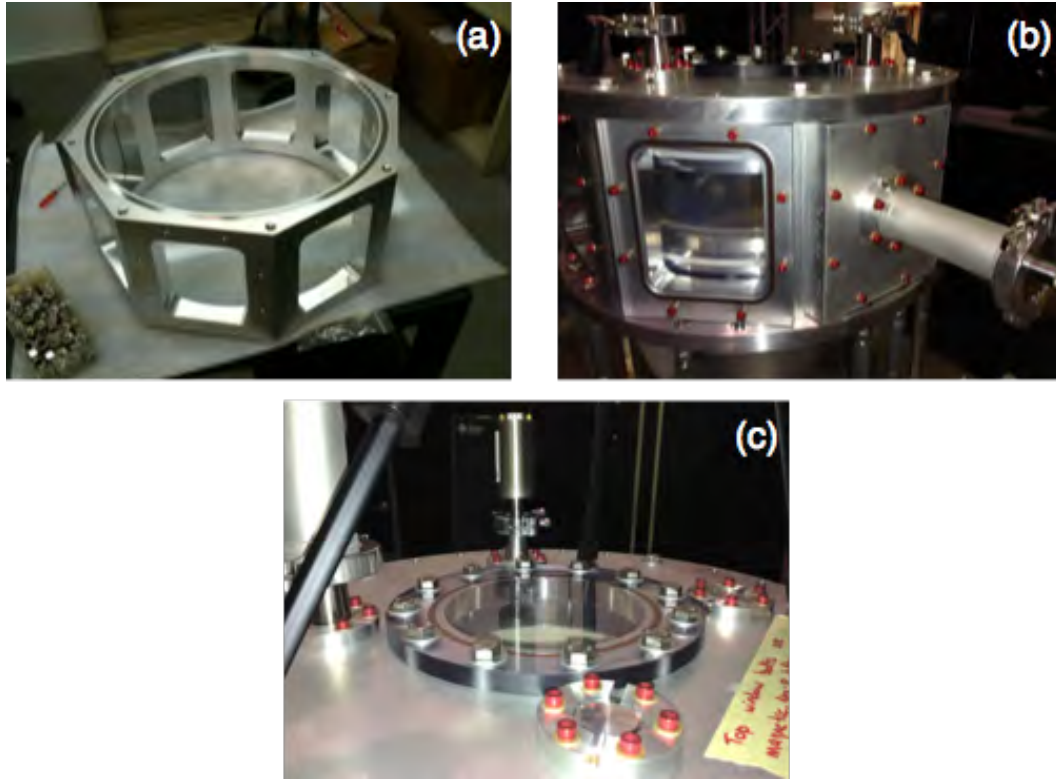


Figure 5: Views of the MDPX vacuum chamber. (a) the octagonal frame of the vacuum chamber prior to adding the top and bottom flanges; (b) side view of the assembled vacuum chamber showing the top and bottom flanges, a window, and a side flange that is adapted to a QF40 nipple – the top and bottom electrodes used for plasma generation are also visible through the side window; (c) top view of the vacuum chamber showing a circular, top viewport and the adaptors to QF25 feedthroughs.

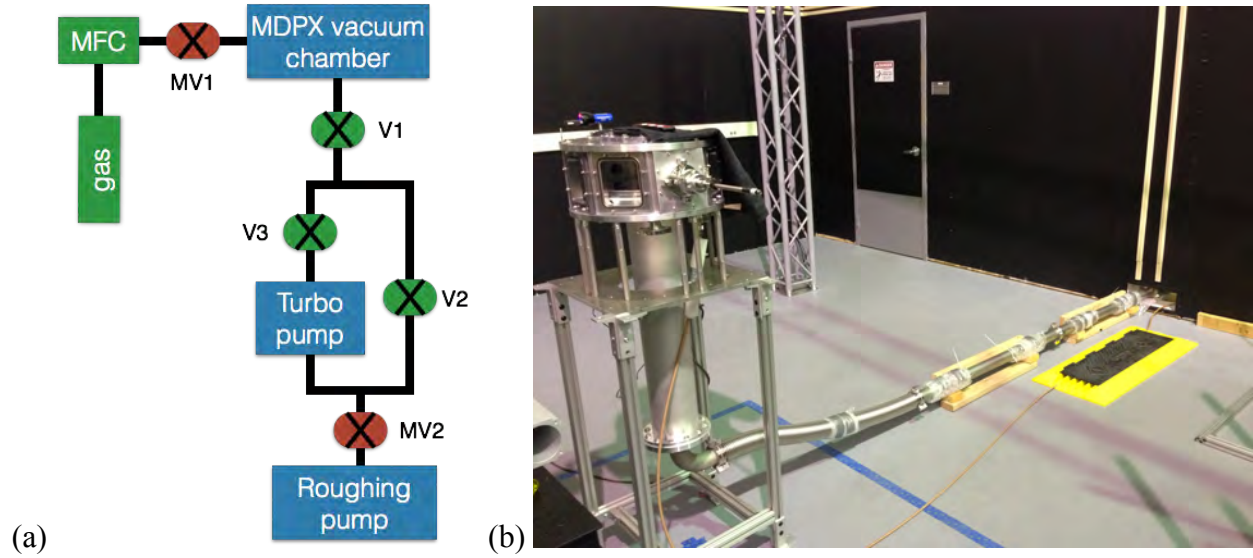


Figure 6 (a) Schematic layout of the MDPX vacuum system. The valves V1, V2, and V3 are pneumatic valves that are remotely controlled by a *LabVIEW* control program. The valves MV1 and MV2 are manual valves. (b) A photograph of the octagonal vacuum chamber with a lower extension on a test stand, prior to the delivery of the magnet. The ISO63 tubing to the pumping station is shown running along the floor of the laboratory.

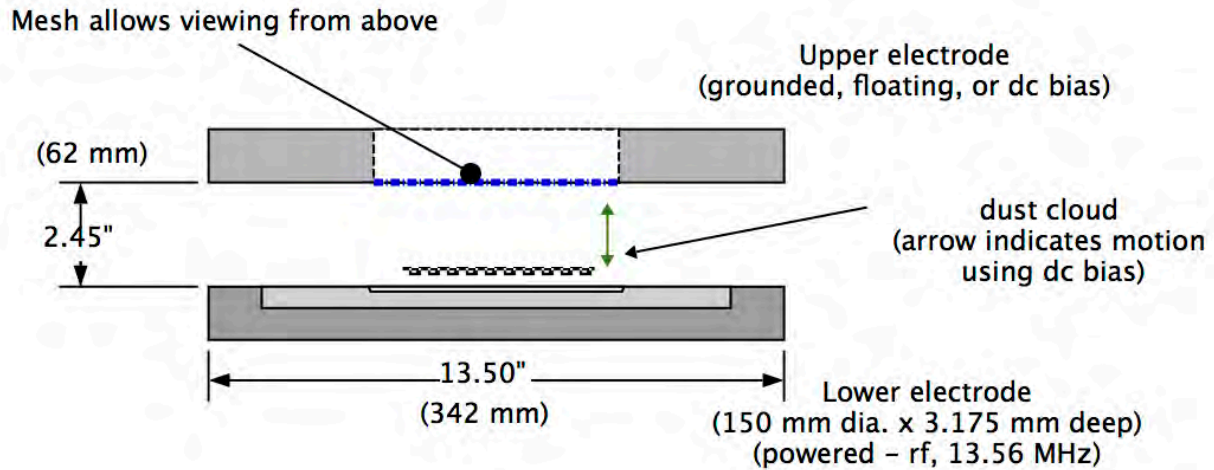


Figure 7: (a) Schematic layout of the MDPX vacuum system. The valves V1, V2, and V3 are pneumatic valves that are remotely controlled by a *LabVIEW* control program. The valves MV1 and MV2 are manual valves. (b) A photograph of the octagonal vacuum chamber with a lower extension on a test stand, prior to the delivery of the magnet. The ISO63 tubing to the pumping station is shown running along the floor of the laboratory.

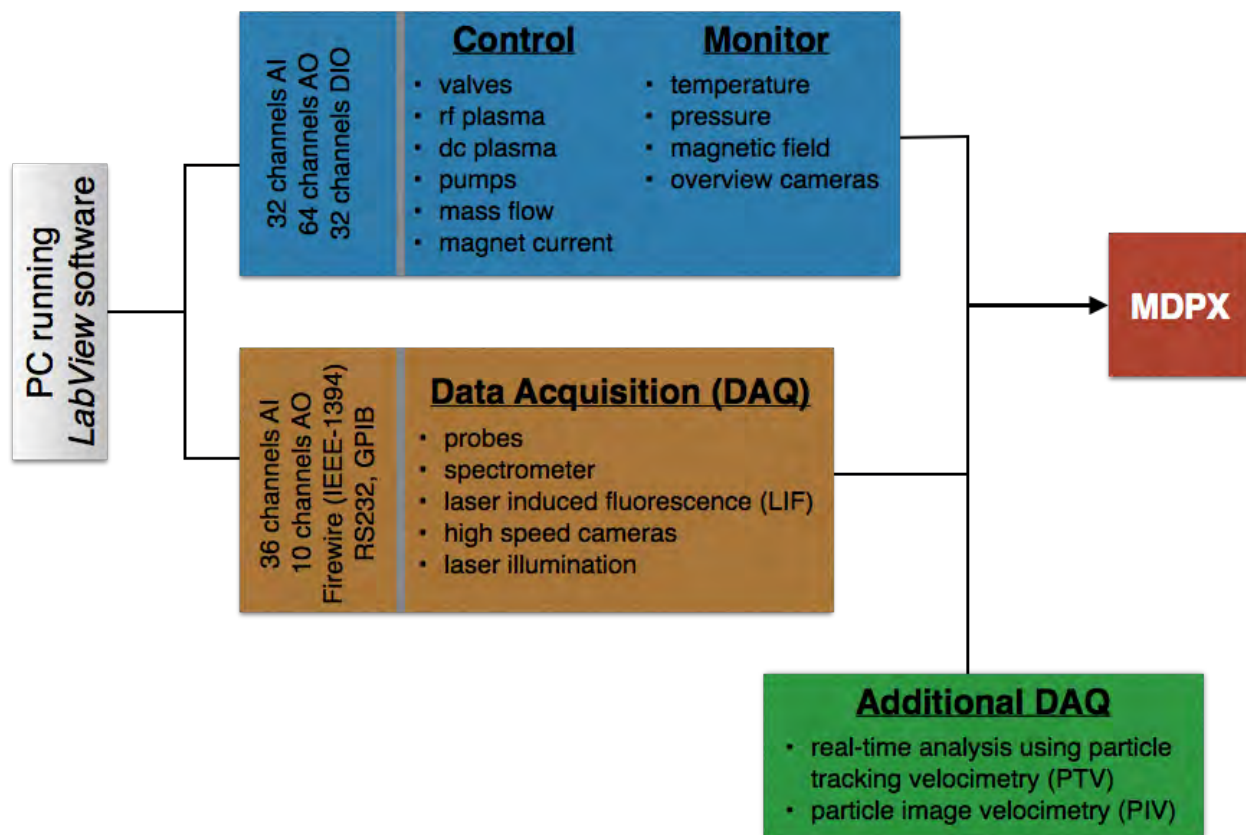


Figure 8: Schematic layout of the experimental control/monitoring and data acquisition system. The overall system is controlled by a PC running *LabVIEW* software. On the control and monitoring side, 32 channels of analog input (AI), 64 channels of analog output (AO) and 32 channels of digital input/output (DIO) are used to provide continuous monitoring of the “operating state” of the experiment. This information is acquired at data rates between 250 and 800 kSamples/s. For data acquisition of research data, measurements are performed at rates typically between 1 and 4 MSamples/s. Data can also be acquired through Firewire, RS232, and GPIB interfaces.



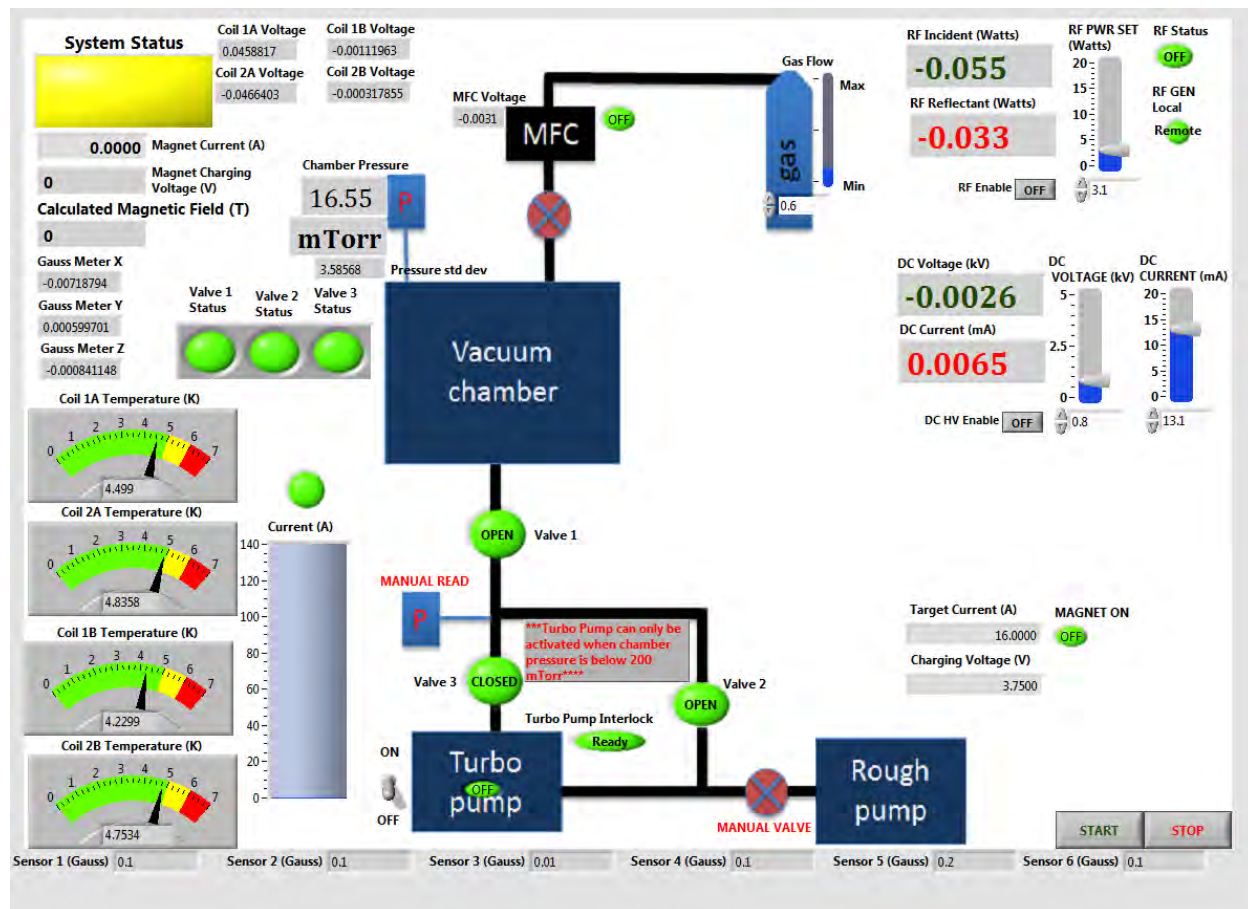


Figure 9: A snapshot of the primary *LabVIEW* front panel from the control computer. Shown in this single panel are indicators (temperature and magnetic field) and controls (magnet current and charging voltage) for the magnet, controls for rf and dc power supplies, and controls and indicators for the vacuum and gas systems.

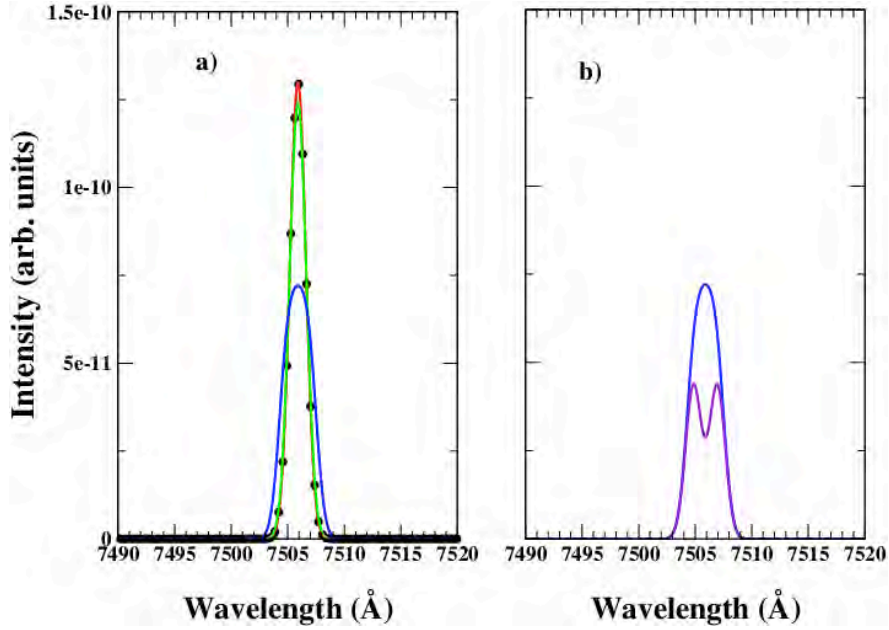


Figure 10: Effect of magnetic fields on the line emission from Ar I. Data from four different magnetic field ( $B$ ) cases are shown:  $B = 0, 0.1, 1$ , and  $4$  T. (a) Shows the total emission in the line (both linearly and circularly polarized light). The black circles are the zero-field results, the red line is the 1000 Gauss result, the green line is the 1 T and the blue is the 4 T. (b) Shows just the 4 T results. The blue line is the total and the purple line is just the circularly polarized signal. The transition is  $3s^2 3p^5 4p (^1S_0) \rightarrow 3s^2 3p^5 4s (^1P_1)$ . [Calculation by S. Loch, Auburn University].



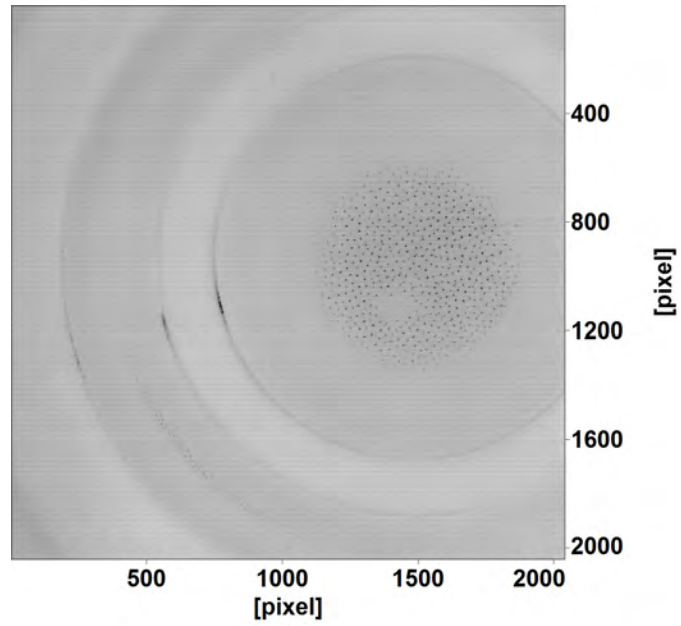


Figure 11: Image of a dust cloud of 8-micron diameter microparticles suspended in an argon plasma at a magnetic field of 2 Tesla in the MDPX device.

- <sup>1</sup> F. F. Chen, *Introduction to Plasma Physics and Nuclear Fusion*, ()
- <sup>2</sup> R. J. Goldston and P. H. Rutherford, *Introduction to Plasma Physics*, Institute of Physics Publishing, London, (1997), p. 19.
- <sup>3</sup> M. G. Kivelson, "Physics of Space Plasmas", in *Introduction to Space Physics*, eds. M. G. Kivelson and C. T. Russell, Cambridge University Press, p. 27 (1995).
- <sup>4</sup> K. Miyamoto, *Plasma Physics for Nuclear Fusion – Revised Edition*, The MIT Press, Cambridge, MA, (1987), p. 12.
- <sup>5</sup> P. K. Shukla and A. A. Mamun, *Introduction Dusty Plasma Physics*, Institute of Physics Publishing, London, 2002), p. 36.
- <sup>6</sup> I. Langmuir, C. Found, and A. Dittmer, "A NEW TYPE OF ELECTRIC DISCHARGE: THE STREAMER DISCHARGE," *Science*, **60**, 392, (1924).
- <sup>7</sup> L. Mestel and L. Spitzer Jr, "Star Formation in Magnetic Dust Clouds," *Mon. Not. R. Astron. Soc.*, **116**, 503, (1956).
- <sup>8</sup> D. Gurnett, E. Grün, D. Gallagher, W. Kurth, and F. Scarf, "Micron-Sized Particles Detected near Saturn by the Voyager Plasma Wave Instrument," *Icarus*, **53**, 236, (1983).
- <sup>9</sup> C. Goertz and G. Morfill, "A model for the formation of spokes in Saturn's ring," *Icarus*, **53**, 219 (1983).
- <sup>10</sup> C. Goertz, "Dusty plasmas in the solar system," *Rev. Geophys. and Space Phys.*, **27**, 271 (1989).
- <sup>11</sup> G. Selwyn, J. Singh, and R. Bennett, "In situ laser diagnostic studies of plasma-generated particulate contamination," *J. Vac. Sci. Technol. A: Vacuum*, **7**, 2758 (1989).
- <sup>12</sup> G. Selwyn, J. McKillop, K. Haller, and J. Wu, "In situ plasma contamination measurements by HeNe laser light scattering: A case study," *J. Vac. Sci. Technol. A: Vacuum*, **8**, 1726 (1990).
- <sup>13</sup> A. Barkan, R. L. Merlino, N. D'Angelo, "Laboratory observation of the dust-acoustic wave mode," *Phys. Plasmas*, **2**, 3563 (1995).
- <sup>14</sup> A. Piel, V. Nosenko, and J. Goree, "Laser-excited shear waves in solid and liquid two-dimensional dusty plasmas," *Phys. Plasmas*, **13**, 042104 (2006).
- <sup>15</sup> H. Thomas, G. E. Morfill, V. Demmel, J. Goree, B. Feuerbacher, and D. Mölmann, "Plasma Crystal: Coulomb crystallization in a dusty plasma", *Phys. Rev. Lett.*, **73**, 652 (1994).
- <sup>16</sup> J. H. Chu and Lin I, "Direct observation of Coulomb crystals and liquids in strongly coupled rf dusty plasmas", *Phys. Rev. Lett.*, **72**, 4009 (1994).
- <sup>17</sup> M. Rosenberg, R. Merlino, and P. K. Shukla, "On the possibility of refraction of dust acoustic waves," *J. Plasma Phys.*, **77**, 231 (2011).
- <sup>18</sup> E. Thomas, Jr., R. L. Merlino and M. Rosenberg, "Magnetized Dusty Plasmas: the Next Frontier for Complex Plasma Research", *Plasma Phys. Control. Fusion*, **54**, 4034 (2012).
- <sup>19</sup> M. M. Vasiliev, L. G. D'yachkov, S. N. Antipov, R. Huijink, O. F. Petrov, and V. E. Fortov, "Dynamics of dust structures in a dc discharge under action of axial magnetic field," *EPL (Europhys. Lett.)*, **93**, 15001 (2011).
- <sup>20</sup> N. Sato, G. Uchida, T. Kaneko, S. Shimizu, and S. Iizuka, "Dynamics of fine particles in magnetized plasmas," *Phys. Plasmas*, **8**, 1786 (2001).
- <sup>21</sup> U. Konopka, M. Schwabe, C. Knappek, M. Kretschmer, and G. E. Morfill, "Complex Plasmas in Strong Magnetic Field Environments", in *New Vistas in Dusty Plasmas: Fourth International Conference on the Physics of Dusty Plasmas*, eds. L. Boufendi, M. Mikkian, and P. K. Shukla, AIP Press, CP799, p. 181 (2005).

- 
- <sup>22</sup> M. Schwabe, U. Konopka, P. Bandyopadhyay, and G. E. Morfill, "Pattern Formation in a Complex Plasma in High Magnetic Fields," *Phys. Rev. Lett.*, **106**, 215004 (2011).
- <sup>23</sup> S. Knist, F. Greiner, F. Biss, and A. Piel, "Influence of Negative Ions on Drift Waves in a Low-Density Ar/O<sub>2</sub>-Plasma," *Contrib. Plasma Phys.*, **51**, 769 (2011).
- <sup>24</sup> K. DeBleeker, A. Bogaerts, and W. Goedheer, "Role of the thermophoretic force on the transport of nanoparticles in dusty silane plasmas", *Phys. Rev. E*, **71**, 066405 (2005)
- <sup>25</sup> Ch. Deschenaux, A. Affolter, D. MAgni, Ch. Hollenstein, and P. Fayet, "Investigations of CH<sub>4</sub>, C<sub>2</sub>H<sub>2</sub> and C<sub>2</sub>H<sub>4</sub> dusty RF plasmas by means of FTIR absorption spectroscopy and mass spectrometry", *J. Phys. D: Appl. Phys.*, **32**, 1876 (1999).
- <sup>26</sup> F. Greiner, J. Carstensen, N. Köhler, I. Pilch, H. Ketelsen, S. Knish, and A. Piel, "Imaging Mie ellipsometry: dynamics of nanodust clouds in an argon–acetylene plasma", *Plasma Sources Sci. Technol.*, **21**, 065005 (2012).
- <sup>27</sup> N. Rynn and N. D'Angelo, "Device for Generating a Low Temperature, Highly Ionized Cesium Plasma," *Rev. Sci. Instrum.*, **31**, 1326 (1960).
- <sup>28</sup> C Thompson, A. Barkan, N. D'Angelo, and R. L. Merlino, "Dust Acoustic Waves in a Direct Current Glow Discharge", *Phys. Plasmas*, **4** (1997), 2331.
- <sup>29</sup> A. C. Eadon, E. Tejero, A. DuBois, and E. Thomas, "Upgrades to the Auburn Linear Experiment for Instability Studies", *Rev. Sci. Instrum.*, **82**, 063511 (2011).
- <sup>30</sup> A. M. DuBois, A. C. Eadon, and E. Thomas, 'Electron-Ion Hybrid Instability Experiment Upgrades to the Auburn Linear Experiment for Instability Studies', *Rev. Sci. Instrum.*, **84**, 043503 (2013).
- <sup>31</sup> M. Ciancesa, "Measurements and modifications of sheared flows and stability on the Compact Toroidal Hybrid stellarator", Ph.D. dissertation, Auburn University (2012).
- <sup>32</sup> **I. H. Hutchinson, Introduction to Plasma Diagnostics, [Finish Reference].**
- <sup>33</sup> **ADD TEXT**
- <sup>34</sup> Ph. Verplancke, R. Chodura, J.-M. Noterdaeme, and M. Weinlich, "Characteristics of a Langmuir Probe in a Magnetic Field with High Sweep Frequencies", *Contrib. Plasma Phys.*, **36**, S145, (1996).
- <sup>35</sup> R. Adrian, "Twenty Years of Particle Image Velocimetry", *Experiments in Fluids*, **39**, 159 (2005).
- <sup>36</sup> E. Thomas, "Direct Measurements of Two-Dimensional Velocity Profiles in Direct Current Glow Discharge Dusty Plasmas", *Phys. Plasmas*, **6**, 2672 (1999).
- <sup>37</sup> E. Thomas, Jr., J. D. Williams, and J. Silver, "Application of stereoscopic particle image velocimetry to studies of transport in a dusty (complex) plasma," *Phys. Plasmas*, **11**, L37 (2004).
- <sup>38</sup> J. Williams and E. Thomas Jr., "Initial measurement of the kinetic dust temperature of a weakly coupled dusty plasma," *Phys. Plasmas*, **13**, 063509 (2006).
- <sup>39</sup> DaVis (Data Visualization) software, Version 8.0, LaVision GmbH (Göttingen, Germany, 2013).
- <sup>40</sup> V. N. Tsytovich, N. Sato, and G. E. Morfill, *New J. Phys.*, **5**, 43 (2003).
- <sup>41</sup> J. S. Chang and K. Spariosu, "Dust particle charging characteristics under a collisionless magneto-plasma," *J. Phys. Soc. Japan*, **62**, 97 (1993).
- <sup>42</sup> C. O. Thompson, N. D'Angelo, and R. L. Merlino, "The interaction of stationary and moving objects with dusty plasmas," *Phys. Plasmas*, **6**, 1421 (1999).
- <sup>43</sup> E. Thomas Jr., K. Avinash, and R. L. Merlino, "Probe induced voids in a dusty plasma," *Phys. Plasmas*, **11**, 1770 (2004).

- 
- <sup>44</sup> U. Konopka, G. E. Morfill and L. Ratke, "Measurement of the Interaction Potential of Microspheres in the Sheath of a Rf Discharge", *Phys. Rev. Letters*, **84**, 891 (2000).
- <sup>45</sup> S. A. Khrapak, A. V. Ivlev, G. E. Morfill, and S. Zhdanov, "Scattering in the Attractive Yukawa Potential in the Limit of Strong Interaction", *Phys. Rev. Letters*, **90**, 225002 (2003).
- <sup>46</sup> M. Nambu, M. Salimullah, and R. Bingham, "Effect of a magnetic field on the wake potential in a dusty plasma with streaming ions," *Phys. Rev. E*, **63**, 056403 (2001).
- <sup>47</sup> M. Salimullah, M. Torney, P. K. Shukla, and A. K. Banerjee, "Three-Dimensional Wavefields in a Magnetized Dusty Plasma with streaming ions", *Phys. Scripta*, **67**, 534 (2003).
- <sup>48</sup> M. Rosenberg, "Ion- and dust-acoustic instabilities in dusty plasmas", *Planet. Space Sci.* **41**, 229 (1993).
- <sup>49</sup> N. Mitchell, D. Bessette, R. Gallix, C. Jong, J. Knaster, P. Libeyre, C. Sborchia, and F. Simon, "The ITER Magnet System", *IEEE Trans. Appl. Superconductivity*, **18**, 435 (2008).